J Intell Robot Syst (2018) 91:413–424
https://doi.org/10.1007/s10846-017-0734-z

Dynamic Modeling of a Class of Continuum Manipulators in Fixed Orientation

Ammar Amouri[1] · Abdelouahab Zaatri[1] · Chawki Mahfoudi[2]

Received: 30 May 2017 / Accepted: 19 October 2017 / Published online: 28 October 2017

Abstract The current research topic on modeling continuum manipulators are shifting toward the development of accurate dynamic models by considering more specificities and mechanical properties. In this paper, we present a dynamic modeling of a class of continuum manipulators namely driving-cables robots based on the Euler-Lagrange method. The dynamic model is developed based on the kinematic equations of inextensible bending section with zero torsion and by using the constant curvature assumption. Taylor expansion has been applied to the geometric model in order to avoid singularities and reduce the complexity of the mathematical expressions. At the end, some simulation results are presented showing the static equilibrium as well as the dynamic behavior. In addition, a classic Proportional-Integrated-Derivative (PID) controller is proposed to ensure tracking trajectories using the point-to-point technique.

Keywords Continuum manipulator · Driving-cables robot · Dynamic modeling · Euler-lagrange equations · Taylor expansion approximation · PID controller

✉ Abdelouahab Zaatri
azaatri@yahoo.com

Ammar Amouri
ammar_amouri@yahoo.fr

Chawki Mahfoudi
mahfoudi.chawki@gmail.com

[1] Department of Mechanical Engineering, Faculty of Engineering Sciences, University of Brothers Mentouri, Constantine, Algeria

[2] Department of Mechanical Engineering, University Labri Ben M'Hidi Oum el Bouaghi, Oum El Bouaghi, Algeria

1 Introduction

Continuum manipulators have a complex structure and theoretically infinite degrees of freedom. They are inspired from biologic systems found in nature [1–3]. Their actuations are carried out by cables, tendons or pneumatic sources instead of mechanical actuators [4–8]. These manipulators are particularly adapted for exploration and inspection of very confines environments [9, 10], and are most suitable for handling specific applications such as medical and surgical applications [11].

Concerning the kinematic modeling, continuum manipulators are often kinematically redundant and expressed with highly nonlinear terms. These facts make their modeling and control more difficult. However, these manipulators can be modeled and practically controlled only by considering a finite number of degrees of freedom [1]. The most adapted kinematic approaches consider the whole of continuum manipulator as a real or virtual backbone curve depending on the considered robot structure [12]. Some recent contributions and approaches have been proposed to solve kinematics modeling for both single bending section and multi -bending sections of continuum manipulator based on reasonable kinematics assumptions and using some approximations [12–18].

Concerning the dynamic modeling of continuum manipulators, in order to obtain more realistic comportment, the most adapted approaches attempt to include as much as possible more specificities and mechanical properties. To the best of our knowledge, the first research in this field has been introduced in [19], which has considered an approximation of the dynamics of hyper-redundant manipulator as continuum arcs using the modal approach. This model has been calculated by three different methods such as Lagrange and Newton-Euler. Generally, there are a considerable number

of researches on dynamic modeling of these manipulators [20–24]. In reference [20], the authors have formulated an approximation of the dynamics of hyper-redundant manipulator as a continuum mechanics problem. This model is based on the geometric model of extensible continuum robot manipulator with zero torsion. Another dynamic model for spatial multiple sections continuum manipulators has been presented in [21]. This model is based on some assumptions such as constant curvature and concentrated masses. Another dynamic model of a class of continuum manipulators, called Bionic Handling Assistant, is presented in [22]. This model is developed by using the Euler-Lagrange formalism and is based on some assumptions such as constant curvature kinematics and concentrated masses situated on the head coordinate frame of each bending section. Again, another dynamic model of variable length multi-section continuum arms is presented in [23]. This later model is based on circular arc deformation assumption without torsion.

According to the reviewing of the state of the art, we will focus on a specific continuum manipulator called driving-cable robot which will be the topic of our research contribution. The particular constitution of this kind of continuum manipulators is its elastic backbone structure with disks and cables or tendons. To our best knowledge, there are very few work approaches concerning the dynamic modeling compared to its kinematics modeling [24–27]. In reference [24], the authors have presented the dynamic model of a single section for a cable driven continuum manipulator using the Kane's method. This model is derived to account a several parameters such as friction. The same authors extended this model for multi-segment rod-driven continuum robots [25]. Nevertheless, we consider that the resulting models are numerically complex and more difficult to be implemented for control purposes. In reference [26], the authors have presented a dynamic model of a specified continuum robot with single section by using Lagrange method. We have noticed that this model is specified for a robot with only one bending section and therefore cannot be extended to multi-bending sections robot. The dynamic model presented in [27] was derived by Hamilton's principle and based on an appropriate planar large-deflection, but the resulting dynamic model cannot be generalized in three-dimensional case.

Concerning the topic of continuum manipulators control depending on the developed dynamical models, it is a complex research topic but that attracts actually many researchers. Although, the field of manipulators control is in general a very rich topic and presents various control techniques adapted to different structures, but there are few contributions in the field of continuum manipulators. Many contributions have been made on rigid and continuum manipulators including adaptive Neural Networks (NNs), fuzzy, etc; which can be suitable for nonlinear, complex, unknown models under uncertainties and disturbances [28–37]. In reference [28], the authors used an adaptive NN controller allowing accurate tracking of trajectories inside the identified workspace. In reference [29], the authors have proposed an adaptive NN control for parallel manipulators. In references [30–32], composite learning control schemes for flexible-link manipulators have been proposed. In reference [30], firstly, the PD control has been used for the internal dynamics with pole assignment; secondly, a composite learning control using neural modeling error has been applied to the unknown dynamics. In reference [31], the NNs have been used to compensate for system uncertainty approximation and the DOB has been used for compound disturbance estimation. In reference [32], the authors have proposed a sliding mode control with NN and DOB for a flexible-link manipulator with uncertainty. According to the simulations performed by the authors, this control scheme has shown a greater performance for trajectory tracking. In reference [33], the authors study the adaptive NN control for an uncertain robot with unknown dynamics. In reference [34], adaptive neural impedance control has been used for robot-environment interaction. In reference [35], the authors have used NN controllers to suppress the vibration of a flexible robotic manipulator with unknown input dead-zone in the actuators. In reference [36], the authors have used neural network controllers to control the balancing and posture of a biped robot.

Concerning continuum manipulators, two examples of controller are proposed [37, 38]. In reference [37], the path tracking control of the Compact Bionic Handling Arm end-effector is performed using an adaptive kinematic control without physical interactions with the environment. In reference [38], the authors have presented a controller designed for continuum robots, which utilizes a neural network feed-forward component to compensate for dynamic uncertainties.

In this paper, we propose the dynamic model of a multi-bending section continuum manipulator, namely driving -cables robot, in a specific orientation. The main first contribution of this paper is the expansion of the geometric model expressions by means of Taylor series. This technique has enabled the avoidance of singularities, leading to the reduction of the dynamic model complexity which becomes easily useable for control. In order to test our proposed dynamic model, a second main contribution has been performed. It consists on the implementation of a PID controller used for tracking trajectories via the point-to-point technique.

The organization of this paper is as follows: in Section 1, an introduction synthesizes the state of the art related to this research topic including kinematics, dynamics modeling and control of continuum manipulators. Then, in Section 2,

a description of the considered continuum manipulator is presented. In Section 3, the proposed geometric and kinematic descriptions are developed. Section 4 describes the proposed dynamic model in more details. Simulation results on static equilibrium, dynamics and control that validate the proposed model are presented and discussed in Section 5. Finally the conclusion and some research perspectives are given in Section 6.

2 Description of the Continuum Manipulator

The continuum manipulator under consideration which corresponds to the scheme design shown in Fig. 1 is composed of two bending sections. Each bending section with two degrees of freedom is composed of three principal elements: elastic backbone, three driving cables and three spacer disks. The spatial motion of each bending section is governed by deflection of the elastic backbone by applying adequate electrical voltages to one or two motors at the same time in order to generate tensions on the cables. The attachment points of three driving cables are situated at equal angle of 120° on all disks, as shown in Fig. 2.

In order to model the continuum manipulator under consideration, the profile of the whole robot is assimilated to a backbone curve which represents the central axis of the manipulator. The backbone curve of each bending section is modeled by an inextensible arc of circle, oriented in space, and parameterized by an arc length L_k, a curvature κ_k, and an orientation angle φ_k. The bending angle θ_k is measured

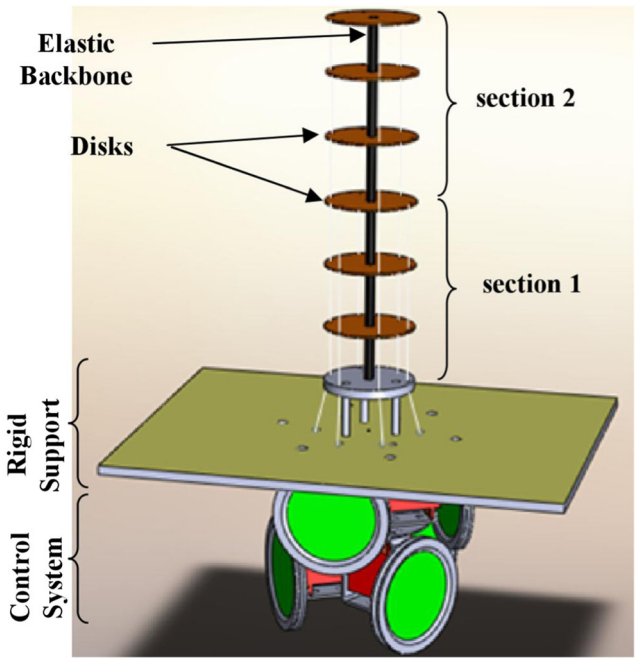

Fig. 1 3D Continuum manipulator design

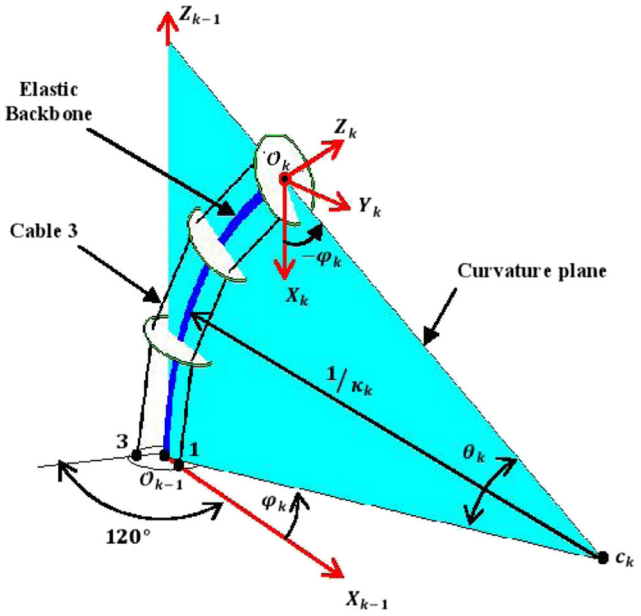

Fig. 2 Circle arc parameters

in curvature plane which is always perpendicular to the $X_{k-1}Y_{k-1}$ plane and rotates around Z_{k-1} axis.

3 Kinematics Analysis

To develop the dynamic model of the continuum manipulator under consideration, the kinematic analyzes, including positions and velocities, are needed and they developed under some assumptions described below:

- The kinematic modeling is based on the constant curvature assumption [3];
- The elastic backbone has a uniform mass distribution along its length;
- The only external force acting on the continuum manipulator is the controlling forces from the cables;
- The elastic backbone is made of materials that possess a high stiffness to avoid possible twisting motions about its axial axis;
- The elastic backbone is assumed to have linear relation between strain and stress [39, 40];
- Each bending section is individually controlled.

Based on the constant curvature assumption, three spaces are used to describe the bending section states. Cables length $\mathbb{Q}_k = [l_i \;\; l_{i+1} \;\; l_{i+2}]^T$, arc parameters $\mathbb{K}_k = [\kappa_k \;\; \theta_k \;\; \varphi_k]^T$ and position/orientation $\mathbb{X}_k = [\mathbf{x}_{p,k} \;\; \mathbf{x}_{o,k}]^T$ representing respectively actuator states, configuration state and task variables. Where $\mathbf{x}_{p,k} = [X_k \;\; Y_k \;\; Z_k]^T$ represents the Cartesian position coordinates, and $\mathbf{x}_{o,k} = [\theta_k \;\; \varphi_k]^T$ represents the orientation coordinates, with bending section index $k = 1, 2$. For simplicity reasons, the index i which

refers to ith cable is assumed that $i = 1$ when $k = 1$ and $i = 4$ when $k = 2$.

The actuator space and the configuration space are associated with a specific transformation to the manipulator robot while transformation from configuration space to task space is independent of the manipulator configuration that focuses mainly on its shape. The global view of kinematics modeling for each bending section is shown in Fig. 3.

3.1 Local Coordinates

In this subsection, the local coordinates, including linear position, orientation, linear velocity and angular velocity, for each bending section are first derived, and the global coordinates are derived thereafter.

The position vector of the endpoint $\mathscr{O}_0$ in the task space $\mathbb{X}_k$ which represents the origin of the frame $\mathscr{R}_k$ can be expressed as a function of configuration space $\mathbb{K}_k$ as follows:

$$\mathbf{r}_k = \begin{cases} x_k = \frac{L_k}{\theta_k}(1-\cos(\theta_k))\cos(\varphi_k) \\ y_k = \frac{L_k}{\theta_k}(1-\cos(\theta_k))\sin(\varphi_k) \\ z_k = \frac{L_k}{\theta_k}\sin(\theta_k) \end{cases} \tag{1}$$

We notice that when θ_k is close to zero, all expressions in Eq. 1 and such equations provided by derivation of this equation become zero divided by zero which leads to numerical singularities. In order to avoid such singularities throughout the analysis, we can use a substitution values when θ_k is close to zero or use other technique such as Taylor expansion.

Here, we will expand the 5th order Taylor expansion with respect to the bending angle θ_k. Thus, Eq. 1 becomes:

$$\mathbf{r}_k = \begin{cases} x_k = \frac{L_k}{24}(-\theta_k^3 + 12\theta_k)\cos(\varphi_k) \\ y_k = \frac{L_k}{24}(-\theta_k^3 + 12\theta_k)\sin(\varphi_k) \\ z_k = \frac{L_k}{120}(\theta_k^4 - 20\theta_k^2 + 120) \end{cases} \tag{2}$$

Since the bending angle θ_k is limited to a small range for this class of continuum manipulators. Then, the bending angle θ_k belongs to the interval $\left[\frac{-3\pi}{5}\ ;\ \frac{3\pi}{5}\right]$, the estimated mean error of the approximation by 5th order of Taylor expansions is less than 1.4%.

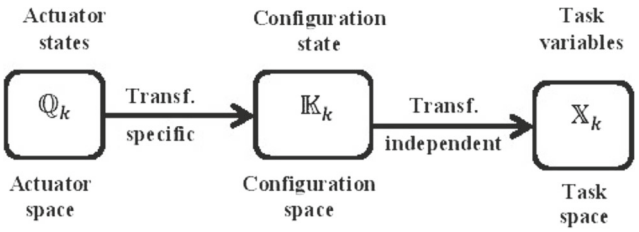

Fig. 3 Global view of the bending section modeling

The orientation of the frame $\mathscr{R}_k$ with respect to frame $\mathscr{R}_{k-1}$ can be defined by three sequential rotations [13]: rotating φ_k around the Z_{k-1} axis, rotating θ_k around the Y_{k-1} axis, and rotating $-\varphi_k$ around the Z_{k-1} axis. The last rotation ensures that the bending section is not subjected to a torsion effect. Thus, the final transformation matrix can be expressed by a rotation matrix $\mathbf{R}_k^{k-1}$, as follows:

$$\begin{aligned} \mathbf{R}_k^{k-1} &= \mathbf{rot}(z_{k-1}, \varphi_k)\ \mathbf{rot}(y_{k-1}, \theta_k)\ \mathbf{rot}(z_k, -\varphi_k) \\ &= \begin{pmatrix} \mathrm{c}^2\varphi_k\mathrm{c}\theta_k + \mathrm{s}^2\varphi_k & \mathrm{c}\varphi_k\mathrm{c}\theta_k\mathrm{s}\varphi_k - \mathrm{c}\varphi_k\mathrm{s}\varphi_k & \mathrm{c}\varphi_k\mathrm{s}\theta_k \\ \mathrm{c}\varphi_k\mathrm{c}\theta_k\mathrm{s}\varphi_k - \mathrm{c}\varphi_k\mathrm{s}\varphi_k & \mathrm{s}^2\varphi_k\mathrm{c}\theta_k + \mathrm{c}^2\varphi_k & \mathrm{s}\varphi_k\mathrm{s}\theta_k \\ -\mathrm{c}\varphi_k\mathrm{s}\theta_k & -\mathrm{s}\varphi_k\mathrm{s}\theta_k & \mathrm{c}\theta_k \end{pmatrix} \end{aligned} \tag{3}$$

where, for instance, the expression $\mathbf{rot}(z_k, \varphi_k)$ means the rotation of the frame $\mathscr{R}_k$ around the Z_{k-1} axis by the angle φ_k, and $\mathrm{c}\theta_k = \cos(\theta_k)$, $\mathrm{s}\theta_k = \sin(\theta_k)$, $\mathrm{c}\varphi_k = \cos(\varphi_k)$ and $\mathrm{s}\varphi_k = \sin(\varphi_k)$.

In order to simplify the calculations, the matrix $\mathbf{R}_k^{k-1}$ is written as a function of unit vectors, as follows:

$$\mathbf{R}_k^{k-1} = [\mathbf{n}_k^{k-1}\ \ \mathbf{b}_k^{k-1}\ \ \mathbf{t}_k^{k-1}] \tag{4}$$

where $\mathbf{n}_k^{k-1}$, $\mathbf{b}_k^{k-1}$ and $\mathbf{t}_k^{k-1}$ are the normal vector, the binormal vector and the tangent vector respectively.

The linear velocity $\mathbf{v}_k$ for the endpoint $\mathscr{O}_k$ can be derived by direct differentiation of Eq. 2 with respect to time as follows:

$$\mathbf{v}_k = \begin{cases} \dot{x}_k = \frac{L_k}{8}(-\theta_k^2 + 4)\dot{\theta}_k\mathrm{c}\varphi_k \\ \qquad -\frac{L_k}{24}(-\theta_k^3 + 12\theta_k)\dot{\varphi}_k\mathrm{s}\varphi_k \\ \dot{y}_k = \frac{L_k}{8}(-\theta_k^2 + 4)\dot{\theta}_k\ \mathrm{s}\varphi_k \\ \qquad +\frac{L_k}{24}(-\theta_k^3 + 12\theta_k)\dot{\varphi}_k\mathrm{c}\varphi_k \\ \dot{z}_k = \frac{L_k}{30}(\theta_k^3 - 10\theta_k)\dot{\theta}_k \end{cases} \tag{5}$$

Based on the motion of the tangent vector of the matrix $\mathbf{R}_k^{k-1}$, the angular velocity ω_k can be defined as follows:

$$\omega_k = \hat{\mathbf{t}}_k^{k-1}\dot{\mathbf{t}}_k^{k-1} \tag{6}$$

where $\dot{\mathbf{t}}_k^{k-1}$ is the derivation vector with respect to time, and $\hat{\mathbf{t}}_k^{k-1}$ is the skew matrix associated with the vector $\mathbf{t}_k^{k-1}$ given by the following matrix:

$$\hat{\mathbf{t}}_k^{k-1} = \begin{pmatrix} 0 & -\mathrm{c}\theta_k & \mathrm{s}\varphi_k\mathrm{s}\theta_k \\ \mathrm{c}\theta_k & 0 & -\mathrm{c}\varphi_k\mathrm{s}\theta_k \\ -\mathrm{s}\varphi_k\mathrm{s}\theta_k & \mathrm{c}\varphi_k\mathrm{s}\theta_k & 0 \end{pmatrix} \tag{7}$$

3.2 Global Coordinates

The vector position of any endpoint $\mathscr{O}_0$ and the rotation matrix of any reference frame $\mathscr{R}_k$ with respect to reference frame $\mathscr{R}_0$ can be calculated recursively as follows:

$$\mathbf{r}_k = \begin{cases} \mathbf{r}_1, & k = 1 \\ \mathbf{r}_1 + \mathbf{R}_1^0\,\mathbf{r}_2, & k = 2 \end{cases} \tag{8}$$

$$\mathbf{R}_2^0 = \mathbf{R}_1^0\,\mathbf{R}_2^1 \tag{9}$$

The linear velocity $\mathbf{v}_k$ for any endpoint can be derived by direct differentiation of Eq. 8 with respect to time as follows:

$$\mathbf{v}_k = \begin{cases} \dot{\mathbf{r}}_1, & k = 1 \\ \dot{\mathbf{r}}_1 + \dot{\mathbf{R}}_1^0\, \mathbf{r}_2 + \mathbf{R}_1^0\, \dot{\mathbf{r}}_2, & k = 2 \end{cases} \tag{10}$$

Also, the angular velocity can be calculated recursively as follows:

$$\omega_k = \begin{cases} \omega_1, & k = 1 \\ \omega_1 + \mathbf{R}_1^0\, \omega_2, & k = 2 \end{cases} \tag{11}$$

4 Dynamics Analysis

The results of the previous section are used here to calculate terms involved in the dynamic model namely the kinetic and potential energies. In the following analysis, the orientation angle φ_k is considered constant (i.e. in fixed orientation).

4.1 Total Kinetic Energy

As mentioned before, the continuum manipulator is composed of elastic backbone, rigid disks and cables. In this study, the masses of elastic backbone, cables and the intermediate disks are neglected. Thus, the total kinetic energy is the sum of translational and rotational energies of the end disks of each bending section, calculated as follows:

$$\mathbf{T} = \sum_{k=1}^{2} (\mathbf{T}_{m_k} + \mathbf{T}_{\mathbf{I}_k}) \tag{12}$$

where the translational and rotational energies of each disk can be calculated respectively, as follows:

$$\mathbf{T}_{m_k} = \frac{1}{2}\, \mathbf{v}_k^T\, m\, \mathbf{v}_k \tag{13}$$

$$\mathbf{T}_{\mathbf{I}_k} = \frac{1}{2}\, \omega_k^T\, \mathbf{I}\, \omega_k \tag{14}$$

where m is the disk's mass, $\mathbf{I}$ is the disk's moment of inertia expressed in the reference frame $\mathscr{R}_0$ which depends on the disk's orientation and local moments of inertia $\mathbf{I}_{xx}$, $\mathbf{I}_{yy}$ and $\mathbf{I}_{zz}$. This moment of inertia can be expressed as follows:

$$\mathbf{I} = (\mathbf{R}_k^0)\, \mathbf{I}_k^k\, (\mathbf{R}_k^0)^T \tag{15}$$

$$\mathbf{I}_k^k = \begin{pmatrix} \mathbf{I}_{xx} & 0 & 0 \\ 0 & \mathbf{I}_{yy} & 0 \\ 0 & 0 & \mathbf{I}_{zz} \end{pmatrix} \tag{16}$$

4.2 Total Potential Energy

The total potential energy for the continuum manipulator is consisting of two parts: the gravitational energy $\mathbf{U}_G$ and the elastic potential energy $\mathbf{U}_E$. Thus, the total potential energy is the sum of these terms given as follows:

$$\mathbf{U} = \mathbf{U}_G + \mathbf{U}_E \tag{17}$$

The gravitational energy of the continuum manipulator depends on the each disk's mass, and can be calculated as follows:

$$\mathbf{U}_G = -\sum_{k=1}^{2} m\, \mathbf{r}_k^T\, g \tag{18}$$

where g is the gravitational constant.

For simplicity reasons, the lengths of two bending sections are equal and they are noted by L. The potential energy of elastic backbones can be calculated as follows [41]:

$$\mathbf{U}_G = \sum_{k=1}^{2} \frac{E\mathbf{I}_b\theta_k^2}{2L} \tag{19}$$

where E is the module of elasticity and $\mathbf{I}_b$ is the second moment of cross-sectional area of each elastic backbone.

4.3 Actuation Forces

For the continuum manipulator under consideration, there are two categories of forces acting on it. One is the controlling force from the cables, and the other is the contact forces between cables and disks resulting in friction forces. In this study the friction forces are neglected.

As mentioned above, the actuation of the continuum manipulator is achieved by pulling one or two cables at the same time for each bending section. Thus, for a spatial motion we can explain tension variations in three cables as a function of orientation angle as presented in Fig. 4.

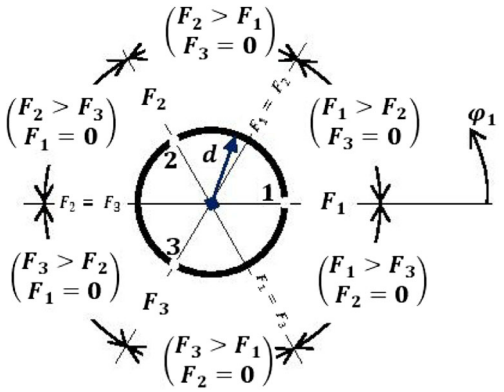

Fig. 4 Scheme showing the tension variations in cables for the first bending section according to the change of the orientation angle φ_1

For instance, let Q_1 be the generalized force acting in the curvature plane of the first bending section in the range as: $\varphi_1 \in [0\ ;\ \frac{2\pi}{3}]$, (see Fig. 4). The relationships between the generalized force Q_1 and cable tensions F_1 and F_2 are given as follows [26]:

$$\begin{cases} Q_1 = F_1\, d\, \cos(\varphi_1) + F_2\, d\, \cos(\frac{2\pi}{3} - \varphi_1) \\ -F_1\, \sin(\varphi_1) + F_2\, \sin(\frac{2\pi}{3} - \varphi_1) = 0 \end{cases} \tag{20}$$

where d is the radial distance between cables and the neutral axis of the continuum manipulator.

With all terms such that the total kinetic energy, the total potential energy and the actuation forces being defined, equations of motion or the dynamic model will be derived in the following.

4.4 Equations of Motion

The second-order partial differential equations in the configuration space are derived using the Euler-Lagrange equations. The motion equations for the continuum manipulator under consideration are given as follows:

$$\frac{d}{dt}\frac{\partial \mathbf{T}}{\partial \dot{\theta}_k} - \frac{\partial \mathbf{T}}{\partial \theta_k} + \frac{\partial \mathbf{U}}{\partial \theta_k} = Q_k, \quad k = 1,\ 2. \tag{21}$$

After developing Eq. 21, the motion equations can be written in the compact form as follows:

$$\begin{bmatrix} M_{11} & M_{12} \\ M_{21} & M_{22} \end{bmatrix} \begin{Bmatrix} \ddot{\theta}_1 \\ \ddot{\theta}_2 \end{Bmatrix} + \begin{bmatrix} C_{11} & C_{12} & C_{13} \\ C_{21} & C_{22} & C_{23} \end{bmatrix} \begin{Bmatrix} \dot{\theta}_1^2 \\ \dot{\theta}_1\dot{\theta}_2 \\ \dot{\theta}_2^2 \end{Bmatrix} + \begin{Bmatrix} K_1 \\ K_2 \end{Bmatrix} = \begin{Bmatrix} Q_1 \\ Q_2 \end{Bmatrix} \tag{22}$$

The elements of matrices described in Eq. 22 are defined in the appendix.

4.5 State Space Representation of the Dynamical Model

To simulate the input-output behavior of the continuum manipulator under consideration, the 4th order Runge-Kutta method is used as a numerical solution. For this, we introduce the state variables as follows:

$$\begin{cases} u_1 = \theta_1(t) \\ u_2 = \dot{\theta}_1(t) \\ u_3 = \theta_2(t) \\ u_4 = \dot{\theta}_2(t) \end{cases} \tag{23}$$

Therefore, by introducing the state variables, Eq. 22 can be written in the general form as follows:

$$\begin{cases} \dot{u_1} = u_2 \\ \dot{u_2} = \frac{1}{M_{11}}(Q_1 - K_1 - C_{13}u_4^2 - C_{12}u_2u_4 - C_{11}u_2^2 \\ \quad - \frac{M_{12}}{M_{12}M_{21} - M_{11}M_{22}}(Q_1M_{21} + K_2M_{11} - Q_2M_{11} \\ \quad - K_1M_{21} - (C_{13}M_{21} - C_{23}M_{11})u_4^2 - (C_{11}M_{21} \\ \quad - C_{21}M_{11})u_2^2 - C_{13}M_{21}u_2u_4)) \\ \dot{u_3} = u_4 \\ \dot{u_4} = \frac{1}{M_{12}M_{21} - M_{11}M_{22}}(Q_1M_{21} - K_2M_{11} - Q_2M_{11} \\ \quad - K_1M_{21} - (C_{13}M_{21} - C_{23}M_{11})u_4^2 - (C_{11}M_{21} \\ \quad - C_{21}M_{11})u_2^2 - C_{13}M_{21}u_2u_4)) \end{cases} \tag{24}$$

Finally, Eq. 24 can be written in the general form as follows:

$$\dot{U}(t) = f(U,t) + g(U,t)H(t) \tag{25}$$

where $U(t)$ represents state variable vector, $f(U,t)$ and $g(U,t)$ are nonlinear functions, and $H(t)$ represents the command vector.

5 Simulation Studies

To simulate the continuum manipulator behavior with two bending sections, the static and the dynamics models have been implemented in MATLAB 7.1. The material and geometric properties of the continuum manipulator under consideration is given in Table 1.

5.1 Simulation of Static Analysis

The simulation of the static analysis considers a continuum manipulator constituted of two bending sections. It is illustrated by an example where the static equilibrium is ensured with zero tensions in the six cables. For this static

Table 1 Parameters of the continuum manipulator

Parameters	Designation	Value
L	bending section length	0.3 m
m	disk mass	0.01 kg
g	gravity constant	9.81 m/s^2
E	Young's modulus	2.1 . 10^{11} Pa
$\mathbf{I}_b$	inertia moment of disk	3.97 . 10^{-12} m^4
$\mathbf{I}_{xx}$	inertia moment of elastic backbone	3.06 . 10^{-7} m^4

model, two cases are analyzed depending on assumed initial conditions of the bending angle θ_k with $k = 1, 2$. For the first case, the initial conditions are $\theta_1 = \frac{\pi}{12}$ and $\theta_2 = 0$; whereas for the second one, the initial conditions are $\theta_1 = 0$ and $\theta_2 = \frac{\pi}{12}$.

The performed simulations of the two cases have provided the corresponding dynamic responses for the bending angles θ_k of the continuum manipulator with zero tension in the six cables as shown on the left-hand side of Fig. 5. It can be seen that each bending section of the continuum manipulator presents oscillations around an equilibrium position (Z_k-axis). For these two cases, the continuum manipulator begins to stabilize after 45 sec and 28 sec, respectively, with a sampling interval of 0.045 sec. For both cases, after release, the starting oscillations of the central axis of the continuum manipulator are shown on the right-hand side of Fig. 5 (blue color for the first bending section and the red color for the second one).

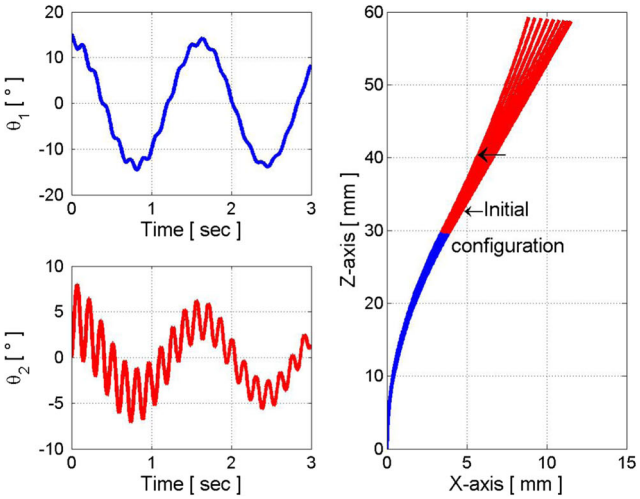

(a) Case 1: initial conditions are: $\theta_1 = \frac{\pi}{12}$ and $\theta_2 = 0$

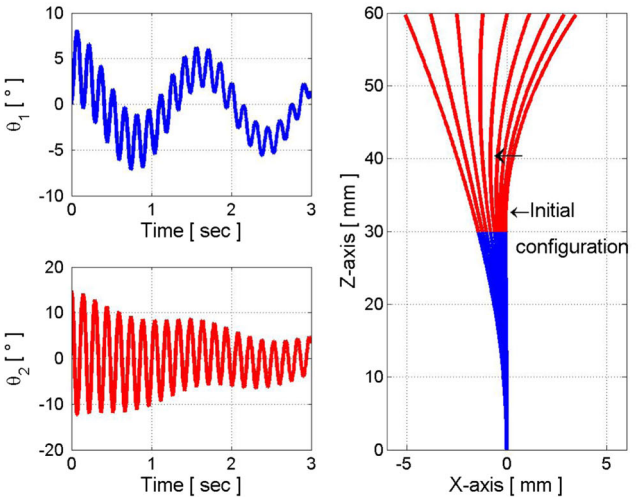

(b) Case 2: initial conditions are: $\theta_1 = 0$ and $\theta_2 = \frac{\pi}{12}$

Fig. 5 Zero actuation response for the bending angle θ_k with $k = 1, 2$

5.2 Simulation of the Dynamic Behavior

In this subsection, we present, through two examples, the results of the performed simulations for the dynamic model of the considered continuum manipulator

In Fig. 6, we present the dynamic responses for the bending angles θ_k in response to a step input of 2 N as a tension in the cable 1 of the first bending section. From the analysis of this figure, it can be seen that the backbone of the continuum manipulator oscillates around a stable position which is different from the vertical initial position of equilibrium. For the first bending section, the stable position is $\theta_1 = 30.66°$; whereas for the second one it stabilizes at $\theta_2 = 2.44°$. The stable position of the second bending angle results due only to the gravitational loading.

In the second example, we applied tensions on the two first cables for both bending sections (see Figs. 1 and 2). The step inputs of generalized forces are $Q_1 = 0.4\,t$ and $Q_2 = 0.8\,t$, respectively, which are acting in the curvature planes oriented by $\varphi_1 = \varphi_2 = \frac{\pi}{6}$ where t is the time variable.

By considering these generalized forces, the tensions on the cables are given as presented in Fig. 7. The dynamic simulation of the considered continuum manipulator behavior is shown in Fig. 8. We noted that these configurations of the continuum manipulator are performed after stabilization of the dynamic model simulation. Figure 9 presents the variation of cable lengths obtained from the performed kinematic simulation.

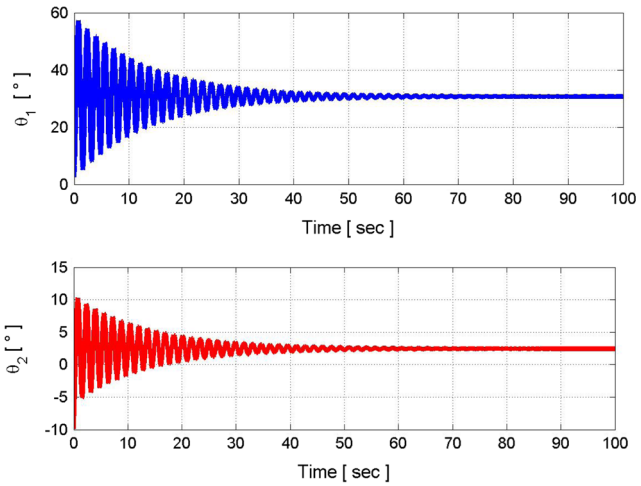

Fig. 6 Dynamic responses for the bending angles θ_k with $k = 1, 2$

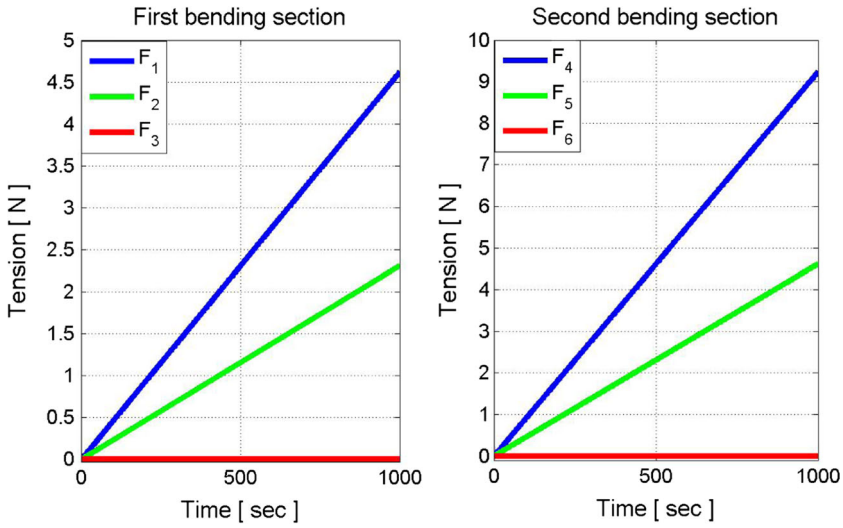

Fig. 7 Temporal evolutions of cable tensions

5.3 Simulation of the PID Controller

After simulation of the proposed dynamic model, we consider two simulation examples of a classical Proportional-Integral-Derivative (PID) controller in order to test the control of the considered continuum manipulator.

The first example represents the response of the proposed PID controller. The resulting value of the dynamic simulation of example 1 is used as input for a PID controller to command the first bending section. The selected parameters of the PID controller which offer an acceptable compromise on performance are: $K_P = 0.1$, $K_i = 2.7$ and $K_d = 0.3$. Figure 10 presents the dynamic response in closed-loop with the PID controller. The observation of the graphical results confirms the possibility to use successfully the proposed controller.

The second example considers the tracking of a circular trajectory in the curvature planes $\varphi_1 = \varphi_2 = 0$. Figure 11 shows the tracking of a circular trajectory with PID controller. The analysis of this figure shows the tracking of a trajectory with acceptable errors. These Euclidean errors are shown on the right-hand side of Fig. 11. The required tensions and cable lengths for the tracking of a circular trajectory are presented in Figs. 12 and 13 respectively.

5.4 Discussion

Although, there is no much works in this particular topic presenting practical results, nevertheless, we have compared our simulation results with references [24] and [26] both to simulations as well as to experiments.

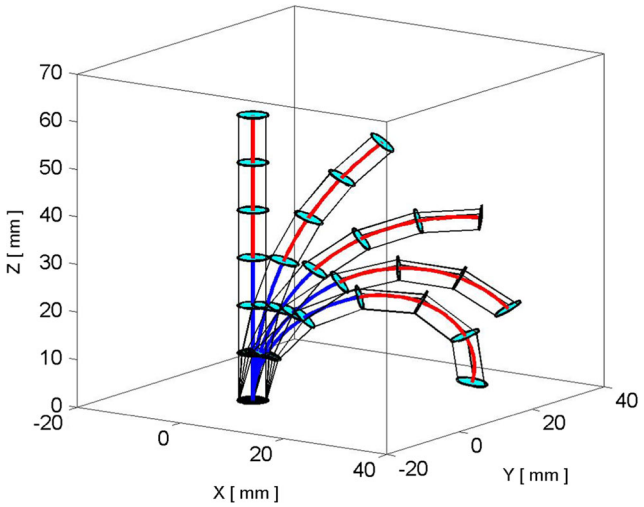

Fig. 8 Some configurations of the continuum manipulator

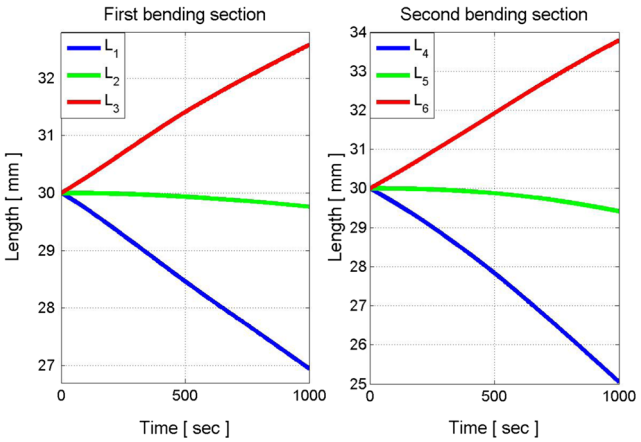

Fig. 9 Temporal evolutions of cable lengths

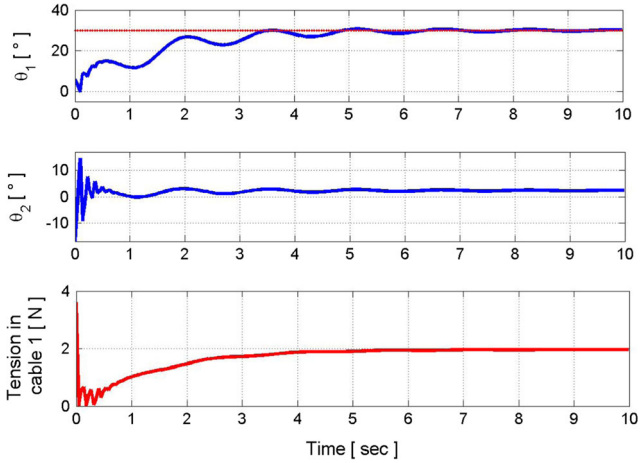

Fig. 10 Dynamic response for the bending angles $\theta_k (k = 1, 2)$ with PID controller and its tension

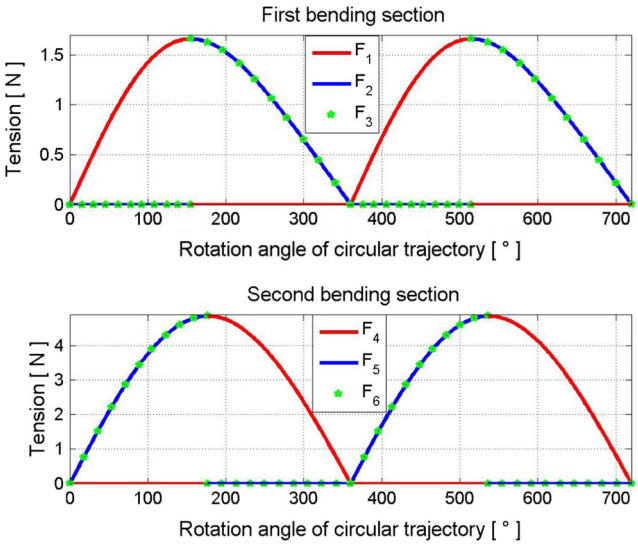

Fig. 12 Evolution of cable tensions

The obtained simulation results for the static and dynamic models show some similarity for dynamic responses of the continuum manipulator behavior when compared to works developed in [24] and [26] despite the differences of initial assumptions, modeling approaches and specificities of the considered continuum manipulators. For instance, our static model and the static model presented in [24] present almost similar results in the case of planar configurations. We observe a very similar shape and behavior between them. In addition, the comparison of our dynamical model with that of [24] shows also some similarities despite the differences in modeling and assumptions since authors have taken into account the friction and the torsion effects.

Concerning the work presented in [26], we notice that their dynamical model outputs some applied forces on the structure which are almost similar to the forces that serve as inputs for our dynamic model. This proves some equivalence between the compared models in terms input-output.

As a general conclusion to our analysis, the comparison of our simulation results to the previous simulation and experimental results leads to validate the proposed dynamic model. Moreover, despite the complexity of our dynamic model due to strong nonlinearities, to some assumed assumptions, and to neglecting the environment perturbations, a classical PID can be fruitfully used for basically testing our model and its control. The obtained results from the performed simulations enable to conclude

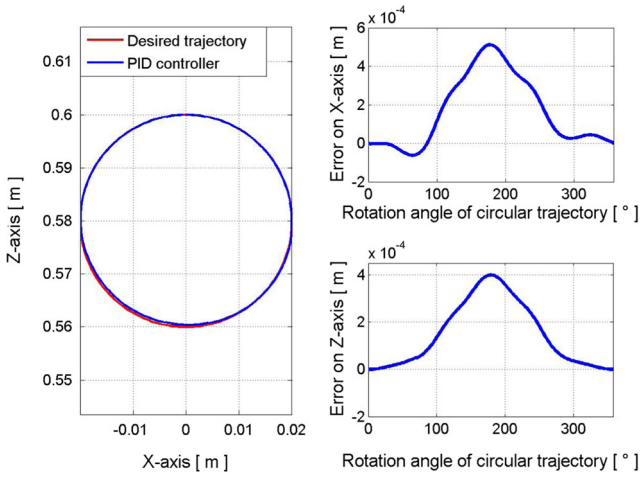

Fig. 11 Tracking of a circular trajectory with PID controller (view in curvature plane)

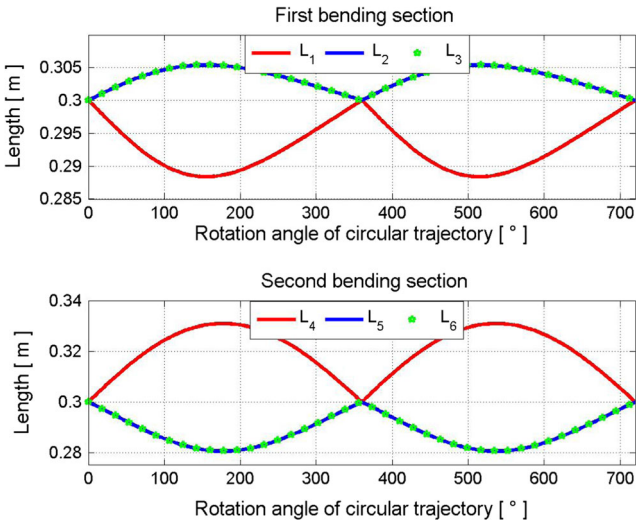

Fig. 13 Evolution of cable lengths

that our dynamic model can be useful for research and implementation purposes.

6 Conclusion

This paper has presented a dynamic model for a class of multi-section continuum manipulators, namely driving-cables robots, in fixed orientation using the Euler-Lagrange method. Firstly, we have exploited Taylor expansion to approximate the geometric model. Deriving the kinematic and dynamic models based on this approximation, we have got two main advantages. The first advantage is the complexity reduction of the mathematical expressions which has enabled an easier analysis and simulation of the system behavior. Moreover, this approach has enabled to avoid some singularities which are initially involved in the geometric model. Under our hypothesis and approximation, the estimation of the error between the initial geometric model and the approximated geometric model by Taylor expansion is less than 1.4 %. Then, we have developed a mathematical formulation defining the bending section kinematics. The dynamical model is derived from the kinematic equations of inextensible bending section with zero torsion. Some simulation examples have been performed for static and dynamic models for the considered continuum manipulator.

Despite the differences of initial assumptions, modeling approaches and specificities of the considered continuum robots, the examination of our simulation results with some simulation and experimental results presented by other authors lead globally to comparable results validating to some extend our dynamic model.

A classic PID controller has been implemented in order to test the proposed dynamic model for controlling the considered continuum manipulator by means of the point-to-point technique. Interesting and coherent results have been obtained even for circular trajectories.

As a perspective, we intend to extend our dynamic model for 3-D space configurations. In will be worthy to take into account the torsion, friction and all gravitational effects in order to approximate the behavior of real continuum manipulators. In addition, the robot control has to be addressed by testing more adapted controllers than the PID one.

Beside basic PID controllers, to expect more efficient control performances while taking into account the complexity, the non linearity, the uncertainties and the perturbations concerning continuum manipulators; it is worthy to implement more advanced and adapted control schemes such as neural networks, sliding mode, fuzzy techniques and eventually their combinations.

Appendix

A Nomenclature

d_k	radial distance between cables and the neutral axis of the bending section
E	Young's modulus
F_i	tension in cable i
g	gravitational constant
i	index of the cable, $i = 1,\ 2,\ 3$.
$\mathbf{I}$	disk's moment of inertia expressed in the reference frame
$\mathbf{I}_b$	inertia moment of elastic backbone
$\mathbf{I}_{xx}$	disk's moment of inertia aligned with x axis
$\mathbf{I}_{yy}$	disk's moment of inertia aligned with y axis
$\mathbf{I}_{zz}$	disk's moment of inertia aligned with y axis
k	index of the bending section
l_i	length of the cable i
L_k	length of the center of the bending section k
m	disk mass
$\mathbf{n}_k,\ \mathbf{b}_k,\ \mathbf{t}_k$	unit vectors of matrix $\mathbf{R}_k^{k-1}$ defining the frame $k-1$ in frame k
Q_k	generalized forces
$\mathbf{r}_k$	position vector of disk k with respect to reference frame
t	time variable
$\mathbf{v}_k$	linear velocity of disk k
κ_k	curvature of the bending section k
φ_k	orientation angle of the curvature plane of the bending section k
θ_k	bending angle in the curvature plane of the bending section k
ω_k	angular velocity of disk k
$\dot{\cdot}$	denoted first derivative with respect to time
$\hat{\cdot}$	denoted skew matrix

B Appendix

Elements of matrices involved in Eq.22.

$$M_{11} = 4\mathbf{I}_{xx} + L^2\left(\frac{\theta_1^4\theta_2^4}{21600} - \frac{\theta_1^4\theta_2^2}{1080} - \frac{\theta_1^3\theta_2^3}{720} + \frac{\theta_1^3\theta_2}{60} - \frac{\theta_1^2\theta_2^4}{720} + \frac{\theta_1^2\theta_2^2}{36} + \frac{\theta_1\theta_2^3}{36} - \frac{\theta_1\theta_2}{3} + \frac{\theta_1^4}{144} - \frac{2\theta_1^2}{9} - \frac{\theta_2^4}{45} - \frac{\theta_2^2}{2} + 5\right)$$

$$M_{12} = M_{21} = 2\mathbf{I}_{xx} + L^2\left(\frac{\theta_1^4\theta_2^4}{51840} - \frac{\theta_1^4\theta_2^2}{2880} - \frac{\theta_1^3\theta_2^3}{1800} + \frac{\theta_1^3\theta_2}{180} - \frac{\theta_1^2\theta_2^4}{1728} + \frac{\theta_1^2\theta_2^2}{96} + \frac{\theta_1\theta_2^3}{90} - \frac{\theta_1\theta_2}{9} + \frac{\theta_1^4}{720} - \frac{\theta_1^2}{24} + \frac{7\theta_2^4}{720} - \frac{5\theta_2^2}{24} + \frac{3}{2}\right)$$

$$M_{22} = 2\mathbf{I}_{xx} + L^2\left(\frac{\theta_2^4}{1440} - \frac{\theta_2^2}{36} + \frac{1}{2}\right)$$

$$C_{11} = L^2\left(\frac{\theta_1^3\theta_2^4}{16200} - \frac{\theta_1^3\theta_2^3}{800} - \frac{\theta_1^3\theta_2^2}{1880} + \frac{\theta_1^2\theta_2}{120} - \frac{\theta_1\theta_2^4}{1080} + \frac{\theta_1\theta_2^2}{72} - \frac{\theta_1^3}{360} + \frac{\theta_1}{18} + \frac{\theta_2^3}{120} - \frac{\theta_2}{18}\right)$$

$$C_{12} = L^2\left(\frac{\theta_1^4\theta_2^3}{6480} - \frac{\theta_1^4\theta_2}{720} - \frac{\theta_1^3\theta_2^2}{300} - \frac{\theta_1^2\theta_2^3}{216} + \frac{\theta_1^2\theta_2}{24} + \frac{\theta_1\theta_2^2}{15} + \frac{\theta_1^3}{90} - \frac{2\theta_1}{9} + \frac{7\theta_2^3}{90} - \frac{5\theta_2}{6}\right)$$

$$C_{13} = \frac{1}{2}C_{12}$$

$$C_{21} = L^2\left(-\frac{\theta_1^4\theta_2^3}{10800} + \frac{\theta_1^4\theta_2}{1080} + \frac{\theta_1^3\theta_2^4}{12960} + \frac{\theta_1^3\theta_2^2}{1440} + \frac{\theta_1^2\theta_2^3}{900} - \frac{\theta_1\theta_2^4}{864} - \frac{\theta_1^2\theta_2}{90} - \frac{\theta_1\theta_2^2}{48} - \frac{\theta_1^3}{360} + \frac{\theta_1}{12} - \frac{\theta_2^3}{30} - \frac{7\theta_2}{18}\right)$$

$$C_{22} = 0$$

$$C_{23} = L^2\left(\frac{\theta_2^3}{720} - \frac{\theta_2}{36}\right)$$

$$K_1 = \frac{E\,\mathbf{I}_b\theta_1}{L} + m\,L\,g\left(-\frac{\theta_1^3\theta_2^4}{720} + \frac{\theta_1^3\theta_2^2}{36} + \frac{\theta_1^2\theta_2^3}{48} - \frac{\theta_1^2\theta_2}{4} + \frac{\theta_1\theta_2^4}{120} - \frac{\theta_1\theta_2^2}{6} - \frac{7\theta_1^3}{30} + \frac{5\theta_1}{3} - \frac{\theta_2^3}{24} + \frac{\theta_2}{2}\right)$$

$$K_2 = \frac{E\,\mathbf{I}_b\theta_2}{L} + m\,L\,g\left(-\frac{\theta_1^4\theta_2^3}{720} + \frac{\theta_1^4\theta_2}{72} + \frac{\theta_1^3\theta_2^2}{48} + \frac{\theta_1^2\theta_2^3}{60} - \frac{\theta_1^2\theta_2}{6} - \frac{\theta_1\theta_2^2}{8} - \frac{\theta_1^3}{12} + \frac{\theta_1}{2} - \frac{\theta_2^3}{30} + \frac{\theta_2}{3}\right)$$

References

1. Robinson, G., Davies, J.B.C.: Continuum robots - A state of the art. In: Proceedings of IEEE International Conference on Robotics and Automation. Detroit, MI, USA (1999)
2. Trivedi, D., Rahn, D.C., Kier, M.W., Walker, D.I.: Soft robotics: Biological inspiration, state of the art, and future research. Appl. Bionics Biomech. **5**(3), 99–117 (2008)
3. Webster III, R.J., Jones, B.A.: Design and kinematic modeling of constant curvature continuum robots: A review. Int. J. Robot. Res. **29**(13), 1661–1683 (2010)
4. Renda, F., Giorelli, M., Calisti, M., Cianchetti, M., Laschi, C.: Dynamic model of a multibending soft robot arm driven by cables. IEEE Trans. Robot. **30**(5), 1109–1122 (2014)
5. Ataka, A., Qi, P., Liu, H., Althoefer, K.: Real-time planner for multi-segment continuum manipulator in dynamic environments. In: IEEE International Conference on Robotics and Automation Stockholm, Sweden (2016)
6. Mahl, T., Hildebrandt, A., Sawodny, O.: Forward kinematics of a compliant pneumatically actuated redundant manipulator. In: IEEE Conference on Industrial Electronics and Applications, pp. 1267–1273 (2012)
7. Laschi, C., Mazzolai, B., Mattoli, V., Cianchetti, M., Dario, P.: Design of a biomimetic robotic octopus arm. Bioinspir. Biomim. **4**(1), 015006 (2009)
8. McMahan, W.B., Jones, A., Walker, I.D.: Design and implementation of a multi-section continuum robot: Air-Octor, pp. 2578–2585 (2005)
9. Davies, J.B.C., Lane, D.M., Robinson, G.C., O'Brien, D.J., Pickett, M., Sfakiotakis, M., Deacon, B.: Subsea applications of continuum robots. In: Proceedings of International Symposium on Underwater Technology. Tokyo, Japan (1998)
10. Buckingham, R., Graham, A.: Nuclear snake-arm robots. Ind. Robot. Int. J. **39**(1), 6–11 (2012)
11. Burgner-Kahrs, J., Rucker, D.C., Choset, H.: Continuum robots for medical applications: a survey. IEEE Trans. Robot. **31**(6), 1261–1280 (2015)
12. Amouri, A., Mahfoudi, C., Zaatri, A., Lakhal, O., Merzouki, R.: A metaheuristic approach to solve inverse kinematics of continuum manipulators. J Syst. Control Eng. **231**(5), 380–394 (2017)
13. Jones, B.A., Walker, I.D.: Kinematics for multi-section continuum robots. IEEE Trans. Robot. **22**, 43–55 (2006)
14. Iqbal, S., Mohammed, S., Amirat, Y.: A guaranteed approach for kinematic analysis of continuum robot based catheter. In: Proceedings of International Conference on Robotics and Biomimetics, pp. 1573–1578. Guilin, China (2009)
15. Hannan, M.W., Walker, I.D.: Kinematics and the implementation of an elephant's trunk manipulator and other continuum style robots. J. Robot. Syst. **20**, 45–63 (2003)
16. Godage, S., Medrano-Cerda, G.A., Branson, D.T., Guglielmino, E., Caldwell, D.G.: Modal kinematics for multi-section continuum arms. Bioinspir. Biomim. **10**, 1–20 (2015)
17. Mahl, T., Hildebrandt, A., Sawodny, O.: A variable curvature continuum kinematics for kinematic control of the bionic handling assistant. IEEE Trans. Robot. **30**(4), 935–949 (2014)
18. Lakhal, O., Melingui, A., Merzouki, R.: Hybrid approach for modeling and solving of kinematics of compact bionic handling assistant manipulator. IEEE/ASME Trans. Mechatron. **21**(3), 1326–1335 (2016)
19. Chirikjian, G.S.: Hyper-redundant manipulator dynamics: a continuum approximation. Adv. Robot. **9**(3), 217–243 (1995)

20. Mochiyama, H., Suzuki, T.: Kinematics and dynamics of a cable-like hyper-flexible manipulator. In: Proceedings of IEEE International Conference on Robotics and Automation, pp. 3672–3677. Taipei, Taiwan (2003)
21. Tatlicioglu, E., Walker, I.D., Dawson, D.M.: New dynamic models for planar extensible continuum robot manipulators. In: Proceedings of IEEE/RSJ International Conference on Intelligent Robots and Systems, pp. 1485–1490. San Diego, USA (2007)
22. Falkenhahn, V., Mahl, T., Hildebrandt, A., Neumann, R., Sawodny, O.: Dynamic modeling of bellows-actuated continuum robots using the Euler-Lagrange formalism. IEEE Trans. Robot. **31**(6), 1–13 (2015)
23. Godage, I.S., Medrano-Cerda, G.A., Branson, D.T., Guglielmino, E., Caldwell, D.G.: Dynamics for variable length multisection continuum arms. Int. J. Robot. Res. **35**(6), 695–722 (2016)
24. Rone, W.S., Ben-Tzvi, P.: Continuum robot dynamics utilizing the principle of virtual power. IEEE Trans. Robot. **30**(1), 275–287 (2014)
25. Rone, W.S., Ben-Tzvi, P.: Mechanics modeling of multi-segment rod-driven continuum robots. J. Mech. Robot. **6**(4), 041006 (2014)
26. He, B., Wang, Z., Li, Q., Xie, H., Shen, R.: An analytic method for the kinematics and dynamics of a multiple-backbone continuum robot. Int. J. Adv. Robot. Syst. **10**, 1–13 (2013)
27. Gravagne, I.A., Rahn, C.D., Walker, I.D.: Large deflection dynamics and control for planar continuum robots. IEEE/ASME Trans. Mechatron. **8**(2), 299–307 (2003)
28. Daachi, B., Madani, T., Benallegue, A.: Adaptive neural controller for redundant robot manipulators and collision avoidance with mobile obstacles. Neurocomputing **79**, 50–60 (2012)
29. Le, T.D., Kang, H.J.: An adaptive tracking controller for parallel robotic manipulators based on fully tuned radial basic function networks. Neurocomputing **137**, 12–23 (2014)
30. Xu, B., Yuan, Y.: Two performance enhanced control of flexible-link manipulator with system uncertainty and disturbances. Sci. China Inf. Sci. **60**(5), 050202:1–050202:11 (2017)
31. Xu, B.: Composite learning control of flexible-link manipulator using NN and DOB. IEEE Transactions on Systems, Man, and Cybernetics: Systems. https://doi.org/10.1109/TSMC.2017.2700433
32. Xu, B., Zhang, P.: Composite learning sliding mode control of flexible-link manipulator. Complexity **2017**(9430259), 6 (2017). https://doi.org/10.1155/2017/9430259
33. He, W., Chen, Y., Yin, Z.: Adaptive neural network control of an uncertain robot with full-state constraints. IEEE Trans. Cybern. **46**(3), 620–629 (2016)
34. He, W., Dong, Y., Sun, C.: Adaptive neural impedance control of a robotic manipulator with input saturation. IEEE Trans. Syst. Man Cybern. Syst. **46**(3), 334–344 (2016)
35. He, W., Ouyang, Y., Hong, J.: Vibration control of a flexible robotic manipulator in the presence of input deadzone. IEEE Trans. Ind. Inf. **13**(1), 48–59 (2017)
36. Sun, C., He, W., Ge, W., Chang, C.: Adaptive neural network control of biped robots. IEEE Trans. Syst. Man Cybern. Syst. **47**(2), 315–326 (2017)
37. Melingui, A., Lakhal, O., Daachi, B., Bosco Mbede, J., Merzouki, R.: Adaptive neural network control of a compact bionic handling arm. IEEE/ASME Trans. Mechatron. **2**(6), 2862–2875 (2015)
38. Braganza, D., Dawson, D.M., Walker, I.D., Nath, N.: A neural network controller for continuum robots. IEEE Trans. Robot. **23**(6), 1270–1277 (2007)
39. Antman, S.S.: Nonlinear problems of elasticity. 107. Springer-Verlag, New York (2005). https://doi.org/10.1007/0-387-27649-1
40. Nemat-Nasser, S., Guo, W.G.: Superelastic and cyclic response of NiTi SMA at various strain rates and temperatures. Mech. Mater. **38**, 463–474 (2006)
41. Fertis, D.G.: Advanced mechanics of structure. Marcel Dekker, Inc., New York City (1996)

Ammar Amouri received his Engineer Degree in Mechanical Engineering in 1995, and his Magister Degree in Mechanical Engineering and Robotics in 2011, both from Labri Ben M'Hidi University, Oum el Bouaghi, Algeria. He received the Ph.D. degree in Mechanical Engineering from the University Constantine 1, Constantine, Algeria, in 2017. Since 2016, he is a lecturer of Mechanical Engineering and robotics at the University of Constantine 1, Algeria. From 2013 to 2016, he was a Researcher at URMA/CRTI Research Center of Industrial Technologies, Annaba, Algeria. His major research focus is on robotic systems modeling.

Abdelouahab Zaatri received his diploma of engineer in Electricity from the University of Louvain at Louvain la Neuve, Belgium in 1981. He received his Ph. D. in Robotics from the Katholieke University Van Leuven, Belgium, in 2000. Since 2000, he is a professor at the University of Constantine 1 and the head of the Laboratory of Advanced Technology Applications (LATA) in Constantine, Algeria. His research interests are oriented toward robotics, human robot interaction, multimodal interfaces, automation, renewable energies, and bio-robotics.

Chawki Mahfoudi was born and lives in Ain Beida, Algeria. He obtained the magister degree in 1997 and he carried its doctorate research investigation from National Polytechnic School of Algiers, Algeria in 2006. He is currently a Professor of mechanical engineering at the faculty of sciences and technology at the university Labri Ben M'Hidi, Oum el Bouaghi, Algeria. His current research interests are Robotics and Mechanics design.